The Astrophysical Journal, 742:109 (14pp), 2011 December 1 doi:10.1088/0004-637X/742/2/109

37 GHz METHANOL MASERS : HORSEMEN OF THE APOCALYPSE FOR THE CLASS II METHANOL MASER PHASE?

S. P. Ellingsen[1,5], S. L. Breen[1,2], A. M. Sobolev[3], M. A. Voronkov[2], J. L. Caswell[2], and N. Lo[4]
[1] School of Mathematics and Physics, University of Tasmania, Private Bag 37, Hobart, TAS 7001, Australia; Simon.Ellingsen@utas.edu.au
[2] CSIRO Astronomy and Space Science, Australia Telescope National Facility, P.O. Box 76, Epping, NSW 1710, Australia
[3] Astronomical Observatory, Ural Federal University, Lenin avenue 51, 620000 Ekaterinburg, Russia
[4] Departamento de Astronomía, Universidad de Chile, Camino El Observatorio 1515, Las Condes, Santiago, Casilla 36-D, Chile
[5] Max-Planck-Institut für Radioastronomie, Auf dem Hügel 69, 53121 Bonn, Germany
Received 2011 August 23; accepted 2011 October 14; published 2011 November 14

ABSTRACT

We report the results of a search for class II methanol masers at 37.7, 38.3, and 38.5 GHz toward a sample of 70 high-mass star formation regions. We primarily searched toward regions known to show emission either from the 107 GHz class II methanol maser transition, or from the 6.035 GHz excited OH transition. We detected maser emission from 13 sources in the 37.7 GHz transition, eight of these being new detections. We detected maser emission from three sources in the 38 GHz transitions, one of which is a new detection. We find that 37.7 GHz methanol masers are only associated with the most luminous 6.7 and 12.2 GHz methanol maser sources, which in turn are hypothesized to be the oldest class II methanol sources. We suggest that the 37.7 GHz methanol masers are associated with a brief evolutionary phase (of 1000–4000 years) prior to the cessation of class II methanol maser activity in the associated high-mass star formation region.

Key words: ISM: molecules – masers – radio lines: ISM – stars: formation

Online-only material: color figure

1. INTRODUCTION

Interstellar masers from a wide variety of molecular transitions are observed toward high-mass star formation regions. In particular, ground-state OH masers, 22 GHz water masers, and 6.7 and 12.2 GHz methanol masers are commonly observed toward such regions. Emission from one or more of these transitions has been observed toward more than 1000 sites within our Galaxy. Methanol masers have been empirically divided into two classes. The class I methanol masers are collisionally pumped and typically associated with weak shocks, such as where outflows interact with the surrounding ambient medium (see Voronkov et al. 2006 for a more detailed discussion). The strongest and most common class I methanol masers are those at 36.2 and 44.1 GHz. Class II methanol masers are radiatively pumped and often associated with OH and/or water masers and infrared sources. The strongest and most common class II methanol masers are observed from the 6.7 and 12.2 GHz transitions. This work focuses solely on class II masers.

In addition to the strong and common class II methanol maser transitions at 6.7 and 12.2 GHz there are a large number which are observed to exhibit maser emission in a smaller number of sources. These sources typically show strong emission in the common transitions and a small number have been investigated in detail and the maser emission modeled (e.g., Cragg et al. 2001; Sutton et al. 2001). Maser pumping models are able to explain the broad properties of the observed maser transitions in that the strong and common transitions are usually strongly inverted over a wider range of physical conditions than the weaker, rarer transitions (Cragg et al. 2002, 2005; Pavlakis & Kylafis 1996a, 1996b). However, in many cases the models predict a wide range of parameter space for which emission from strong, common transitions would be accompanied by one or more rare, weak transitions. If we assume that the models are broadly correct, then this suggests that the physical conditions in the majority of sources correspond to physical conditions which preclude the weak, rare masers. This means that, in theory, by observing a wide variety of maser transitions toward a single source, the relative strength (or absence) of the different transitions can be used to constrain the physical conditions where the maser emission arises. The sources where this technique has been applied in detail have been those which show emission in the largest number of rare OH and methanol transitions: W3(OH) (Cesaroni & Walmsley 1991; Sutton et al. 2001), NGC 6334F, and G345.01+1.79 (Cragg et al. 2001).

Regions which show emission from an unusually large number of the rare, weak maser transitions (e.g., W3(OH), NGC 6334F, G345.01+179) are by definition atypical. They must either correspond to an intrinsically rare type of source, rare geometric orientation, or perhaps more likely to a brief period during the evolution of high-mass star formation regions where the conditions are conducive for emission from a wide range of maser transitions. To better understand the properties of more typical maser regions (those which exhibit emission in a smaller number of methanol maser transitions) we have undertaken a program to search for rare, weak masers toward a larger sample of sources, in particular those showing methanol maser emission in the 107 GHz transition. We have previously searched this sample for the 19.9, 23.1, 85.5, 86.6 and 108.8 GHz class II methanol maser transitions (Val'tts et al. 1999; Ellingsen et al. 2003; Cragg et al. 2004; Ellingsen et al. 2004). Here we present the observations for a further three class II methanol transitions which are at frequencies near 38 GHz toward 70 high-mass star formation regions. There is only one previous published study of these transitions, which detected maser emission toward five sources in the 37.7 GHz transition and toward two sources in the 38.3 and 38.5 GHz transitions (Haschick et al. 1989).

2. OBSERVATIONS

The primary sample in our study to expand our understanding of class II methanol masers in star formation regions was the 25 sources observed to exhibit class II methanol maser emission

in the 107 GHz methanol transition. These sources were identified in searches toward more than 175 methanol maser sources (Val'tts et al. 1995, 1999; Caswell et al. 2000; Minier & Booth 2002). These are labeled as sample A in Table 1. Maser modeling and previous observations suggest that the presence of a 107 GHz methanol maser in these sources makes them more likely to be associated with other rare, weak maser transitions than those sources without an associated 107 GHz maser. With the exception of the three atypical sources previously identified, the majority of the sample is associated with either zero, or one rare, weak methanol maser transition, and so is an intermediate group between the majority of sources which are only observed in one or more of the 6.7 and 12.2 GHz transitions, and the very small number of sources which show maser emission in more than six different methanol transitions. In order to reduce the potential for biases in our search we also included observations of two other groups of sources. Previous 19.9 GHz methanol maser observations suggest that star formation regions with centimeter radio continuum emission and 6.035 GHz excited OH masers may be more likely to host rare, weak methanol masers (Ellingsen et al. 2004), and we observed all sources south of declination 0° meeting these criteria (sample B in Table 1, 26 sources in total). The final sample was a search toward all 6.7 GHz methanol masers with a peak flux density >75 Jy, north of a declination of −15° in the catalog of Malyshev & Sobolev (2003; sample C in Table 1, 17 sources). Due to time constraints G 30.70–0.07 and G 31.28+0.06 (nominally members of sample C) were not observed, while ON1 and DR21(OH) were observed despite not meeting the flux density criteria due to the small number of target sources in that LST range. The total sample comprises 70 sources, the vast majority (66) of which are known 6.7 GHz methanol maser sources. The exceptions are Orion KL, OMC 2 (observed as system test sources at Onsala), and G 240.316+0.071, G 328.307+0.430 (6.035 GHz OH maser sources without an associated 6.7 GHz methanol maser). For some of the sources more accurate positions have recently been published (e.g., Caswell 2009) which show that some of the observed positions were in error by up to 10″. These offsets are of comparable magnitude to the telescope pointing errors and have no measurable effect on the observations; however, it should be noted that the positions listed in Table 1 are in all cases the positions at which the observations were made and in some cases these are no longer the most accurate positions measured for these sources.

In order to search for 37.7 and 38 GHz methanol masers in both the northern and southern hemispheres, two separate observing programs were undertaken. The southern hemisphere observations were carried out with the Australia Telescope National Facility (ATNF) Mopra 22 m radio telescope during 2009 May 30–June 3 and 2011 February 1 and 3. The observations were made with the 7 mm receiver system as a back-up project for periods when the weather was too poor for observations at 3 mm. The system temperature varied between approximately 70 and 240 K during the observations. The Mopra spectrometer (MOPS) was configured with 14 IF bands ("zooms") spread over the frequency range from 33.1 to 40.0 GHz. Each IF band covered 138 MHz, with 4096 spectral channels per band and two orthogonal linear polarizations were recorded. This configuration yields a velocity coverage of approximately 1000 km s^{-1} and velocity resolution of 0.32 km s^{-1} (for a channel spacing of 0.27 km s^{-1}) for unsmoothed spectra. The Mopra telescope has rms pointing errors of <10″ and at 38 GHz the telescope has a half-power beamwidth of 73″ (Urquhart et al. 2010).

The 14 IF bands were arranged to cover a variety of methanol maser and thermal molecular transitions. The four methanol maser transitions observed were the class I $4_{-1} \rightarrow 3_0E$ transition at 36.2 GHz and the $7_{-2} \rightarrow 8_{-1}E$, $6_2 \rightarrow 5_3A^-$, and $6_2 \rightarrow 5_3A^+$ class II transitions at 37.7, 38.3, and 38.5 GHz, respectively. The thermal lines observed included a variety of cyanopolyyne transitions and CH_3CN ($J = 2 - 1$). With the exception of the HC_3N ($J = 4 - 3$) ground-state transition at 36.392 GHz, most of these thermal transitions were not detected or were only detected toward a small number of sources with low signal to noise. In this paper we discuss only the results of the observations of the class II methanol maser transitions, the results for the 36.2 GHz class I maser line, and the thermal emission will be reported in a future publication.

The observations were made as a series of position-switched integrations of approximately 60 s duration, with reference observations offset from the target position by 5′ in declination. The data were processed using the ASAP (ATNF Spectral Analysis Package). Most sources had an on-source integration time of approximately 230 s, with the alignment of the velocity channels for the individual scans carried out during processing. The system temperature for the observations was measured by a continuously switched noise diode. At a frequency of 38 GHz the Mopra telescope has a main beam efficiency of approximately 0.52, which implies a scaling factor of 14 for conversion of the intensity scale from units of antenna temperature to Janskys (Urquhart et al. 2010). The rms noise level in the final spectra (after averaging over polarizations and time, but with no smoothing) varied between 0.4 and 1.6 Jy, with the majority being <0.7 Jy. The weather data for Mopra during the observing period are not available and we have used the weather observation at the ATCA (approximately 100 km away) to estimate the atmospheric opacity. The estimated zenith opacity during the observations varied between 0.06 and 0.09, which implies attenuation of between 6% and 11% for these observations. Taking into account pointing, flux density calibration, and variations in the opacity we estimate the measured flux densities to be accurate to 15%.

Two sources (G 351.581–0.353 and G 336.018–0.827) were accidentally omitted from the 2009 Mopra observations and these were observed using a director's time allocation on 2011 February 1 or 3. We also made an additional observation of G 35.201–1.736 on 2011 February 3.

The northern observations were carried out using the Onsala 20 m telescope during 2005 November 29–December 6 using a high electron mobility transistor receiver operating in the 36.0–49.8 GHz range. The system temperature varied between approximately 150 and 350 K during the observations. The spectrometer was configured with 12.8 MHz bandwidth and 1600 spectral channels for the single polarization recorded. This configuration yields a velocity coverage of approximately 100 km s^{-1} and velocity resolution of approximately 0.06 km s^{-1} for unsmoothed spectra. The observations were made in dual beam switching mode with a frequency of 2 Hz and with reference observations offset from the target position by 11′ in declination. The data were processed using the XS package written by P. Bergman (http://www.chalmers.se/rss/oso-en/observations/data-reduction-software). The on-source integration time varied between 15 and 160 minutes. The system temperature for the observations was measured using the chopper-wheel method.

Table 1
Sources Observed in One or More of the 37.7, 38.3, or 38.5 GHz Class II Methanol Maser Transitions

Source Name	Right Ascension (J2000)	Declination (J2000)	rms (Jy)			Velocity Range (km s^{-1})	Sample	Telescope
			(37.7 GHz)	(38.3 GHz)	(38.5 GHz)			
W3(OH)	02:27:03.8	+61:52:25	0.3*	0.5*	1.1*	−93–7	A	Onsala
Orion KL	05:35:14.5	−05:22:30	0.4*	0.6*	1.2*	−42–58		Onsala
OMC 2	05:35:27.5	−05:09:37	0.7	1.0		−38–62		Onsala
Orion S6	05:35:14.0	−05:24:05	0.7	0.8		−51–49	C	Onsala
G 173.481+2.446	05:39:12.9	+35:45:54	0.6	0.6		−64–36	C	Onsala
G 188.95+0.89	06:08:53.7	+21:38:30	0.8*	0.6	1.1	−39–61	A	Onsala
G 192.600–0.048	06:12:54.5	+17:59:20	0.8	0.7		−46–54	A	Onsala
G 213.71–12.60	06:07:48.0	−06:22:57	0.9	0.7		−38–62	C	Onsala
G 240.316+0.071	07:44:51.9	−24:07:42	1.4	1.3	1.3	−40–160	B	Mopra
G 300.969+1.148	12:34:53.4	−61:39:40	1.9	1.6	1.5	−140–60	B	Mopra
G 309.921+0.479	13:50:41.8	−61:35:10	1.6	1.5	1.5	−160–40	B	Mopra
G 310.144+0.760	13:51:58.5	−61:15:40	0.4	0.4	0.4	−200–100	A	Mopra
G 311.643–0.380	14:06:38.8	−61:58:23	1.4	1.5	1.5	−70–130	B	Mopra
G 318.948–0.196	15:00:55.4	−58:58:53	0.4*	0.5	0.4	−180–120	A	Mopra
G 323.459–0.079	15:29:19.4	−56:31:20	1.6	1.5	1.6	−170–30	B	Mopra
G 323.740–0.263	15:31:45.6	−56:30:50	0.8*	0.4	0.4	−200–100	A	Mopra
G 327.120+0.511	15:47:32.8	−53:52:38	0.4	0.4	0.4	−240–60	A	Mopra
G 328.237–0.547	15:57:58.3	−53:59:22	1.8	1.5	1.5	−150–50	B	Mopra
G 328.307+0.430	15:54:06.5	−53:11:40	1.4	1.4	1.4	−190–10	B	Mopra
G 328.808+0.633	15:55:48.5	−52:43:07	0.5	0.5	0.5	−200–100	A	Mopra
G 330.953–0.182	16:09:52.8	−51:54:56	1.1	1.2	1.1	−190–10	B	Mopra
G 331.542–0.066	16:12:09.1	−51:25:48	0.8	0.8	0.8	−190–10	B	Mopra
G 336.018–0.827	16:35:09.3	−48:46:47	0.6	0.6	0.6	−200–100	A	Mopra[†]
G 337.705–0.053	16:38:29.7	−47:00:35	0.6*	0.6	0.5	−205–95	B	Mopra
G 337.404–0.402	16:38:50.4	−47:28:03	0.5	0.6	0.6	−140–60	B	Mopra
G 338.075+0.012	16:39:39.0	−46:41:28	0.6	0.5	0.5	−205–95	B	Mopra
G 340.054–0.244	16:48:13.9	−45:21:44	0.6	0.7	0.6	−200–100	A	Mopra
G 340.785–0.096	16:50:14.8	−44:42:25	0.6*	0.7	0.6	−250–50	A	Mopra
G 339.884–1.259	16:52:04.8	−46:08:34	0.8*	0.8	0.8	−190–110	A	Mopra
G 345.010+1.792	16:56:47.7	−40:14:26	0.7*	0.7*	0.6*	−170–130	A	Mopra
G 343.929+0.125	17:00:10.9	−42:07:19	0.5	0.5	0.5	−190–110	B	Mopra
G 345.504+0.348	17:04:22.8	−40:44:21	0.7	0.7	0.7	−170–130	A	Mopra
G 345.003–0.223	17:05:10.9	−41:29:06	0.7	0.7	0.7	−170–130	A	Mopra
G 347.628+0.148	17:11:50.9	−39:09:30	0.6	0.5	0.5	−250–50	B	Mopra
G 348.550–0.979	17:19:20.4	−39:03:52	0.7	0.6	0.6	−110–90	B	Mopra
G 348.703–1.043	17:20:04.1	−38:58:30	0.8*	0.7	0.7	−150–150	A	Mopra
NGC 6334F	17:20:53.4	−35:47:00	0.9*	1.0*	1.0*	−150–150	A	Mopra
G 351.775–0.536	17:26:42.7	−36:09:16	0.7	0.6	0.6	−160–140	B	Mopra
G 351.581–0.353	17:25:25.2	−36:12:46	0.5	0.5	0.5	−250–50	B	Mopra[†]
G 353.410–0.360	17:30:26.2	−34:41:45	0.6	0.6	0.6	−170–130	A	Mopra
G 354.724+0.300	17:31:15.5	−33:14:05	1.6	1.6	1.5	−50–250	B	Mopra
G 355.344+0.147	17:33:29.0	−32:47:59	1.3	1.4	1.3	−130–170	B	Mopra
G 3.910+0.001	17:54:38.8	−25:34:42	1.1	0.8	0.7	−130–170	B	Mopra
G 5.885–0.392	18:00:30.4	−24:04:03	0.9	1.0	0.9	−150–150	B	Mopra
G 8.669–0.356	18:06:19.0	−21:37:32	1.3	1.2	1.1	−100–200	B	Mopra
G 9.621+0.196	18:06:14.8	−20:31:32	0.6*	0.6	0.6	−150–150	A	Mopra
	18:06:14.8	−20:31:40	1.7*			−50–50		Onsala
G 10.623–0.384	18:10:28.7	−19:55:49	1.2	1.2	1.1	−150–150	B	Mopra
G 11.904–0.141	18:12:11.5	−18:41:28	1.2	1.4	1.2	−110–190	B	Mopra
G 12.909–0.260	18:14:39.5	−17:52:00	0.4	0.4	0.4	−110–190	A	Mopra
G 15.034–0.677	18:20:24.8	−16:11:34	1.1	1.1	1.2	−130–170	B	Mopra
G 20.23+0.07	18:27:43.9	−11:15:04	1.1	1.2		22–122	C	Onsala
G 23.440–0.182	18:34:39.2	−08:31:24	0.4*	0.4	0.4	0–200	A	Mopra
	18:34:39.0	−08:31:36	1.0	1.3		47–147		Onsala
G 23.010–0.411	18:34:40.4	−09:00:37	0.3	0.3	0.3	−80–220	A	Mopra
	18:34:39.9	−09:00:44	1.0	0.9		26–126		Onsala
G 25.65+1.05	18:34:19.7	−05:59:44	1.0	1.6		−8–92	C	Onsala
G 25.709+0.044	18:38:03.1	−06:24:15	1.2	1.0		45–145	C	Onsala
G 28.201–0.049	18:42:58.2	−04:13:56	1.5	1.4	1.4	−50–250	B	Mopra
	18:42:58.0	−04:14:01	4.9			49–149		Onsala
G 29.950–0.020	18:46:03.6	−02:39:24	0.8	1.1		46–146	C	Onsala
G 32.03+0.05	18:49:38.5	−00:45:29	2.2	1.7		43–143	C	Onsala
G 33.640–0.210	18:53:28.7	+00:31:58	2.2			10–110	C	Onsala
G 37.43+1.50	18:54:17.2	+04:41:09	2.2	1.8		−9–91	C	Onsala
G 35.20–0.74	18:58:13.0	+01:40:33	0.9	1.2		−22–78	C	Onsala

Table 1
(Continued)

Source	Right Ascension	Declination	rms (Jy)			Velocity Range	Sample	Telescope
Name	(J2000)	(J2000)	(37.7 GHz)	(38.3 GHz)	(38.5 GHz)	(km s^{-1})		
G 35.201–1.736	19:01:45.5	+01:13:36	0.5	0.5	0.5	−110–190	A	Mopra
	19:01:45.5	+01:13:29	0.8*	0.9	1.4	−7–93		Onsala
G 43.80–0.13	19:11:53.8	+09:35:46	1.7			−10–90	C	Onsala
G 49.49–0.39	19:23:43.4	+14:30:35	0.8	0.8		9–109	C	Onsala
ON1	20:10:09.2	+31:31:35	0.8	0.8		−35–65	C	Onsala
DR21(OH)	20:39:00.7	+42:22:51	0.6	0.7		−50–50	C	Onsala
G 81.87+0.78	20:38:36.8	+42:38:00	0.5	0.7		−43–57	C	Onsala
G 108.18+5.52	22:28:52.1	+64:13:43	0.6	0.6		−61–38	C	Onsala
Cep A	22:56:18.1	+62:01:49	0.7	0.5		−52–47	A	Onsala
NGC 7538	23:13:45.3	+61:28:11	0.7	0.6		−106–−6	A	Onsala

Notes. No entry in the column means that the source was not observed in that transition (this only applies to the Onsala observations as all transitions were observed simultaneously with Mopra). An asterisk for a transition means that emission was detected in that transition, the reported rms was measured in a line-free region of the spectrum. Further details for the detected sources are contained in Tables 2–4. Mopra observations marked with a † were undertaken on either 2011 February 1 or 3.

At a frequency of 38 GHz the Onsala 20 m telescope has an FWHM of 100″ and the aperture efficiency is approximately 0.53, which implies a scaling factor of 18 for conversion of the intensity scale from units of antenna temperature to Janskys. The rms noise level in the final spectra was typically in the range 0.5–2.2 Jy.

We adopted rest frequencies of 37.703696, 38.293292, and 38.452652 GHz for the $7_{-2} \rightarrow 8_{-1}E$, $6_2 \rightarrow 5_3A^-$, and $6_2 \rightarrow 5_3A^+$ transitions, respectively (Xu & Lovas 1997). Comparing these to the rest frequencies used by Haschick et al. (1989), the values we have adopted are between 10 and 33 kHz lower in frequency. To directly compare the velocities observed by Haschick et al. (1989) with those we have observed, offsets of −0.26, −0.11, and −0.08 km s^{-1} should be added to their values for the velocities of the 37.7, 38.3, and 38.5 GHz emission, respectively. Where we have made such comparisons throughout the paper we have applied these offsets to the values reported for the Haschick et al. (1989) velocities. The uncertainties in the rest frequencies of Xu & Lovas (1997) are around 50 kHz (Müller et al. 2004), which corresponds to a velocity of 0.4 km s^{-1} at 37.7 GHz. The close agreement between the velocity of the 37.7 GHz masers and peaks in other transition (see Section 3) suggests that the adopted frequencies are more accurate than the formal uncertainties for these transitions.

3. RESULTS

We have used the Mopra and Onsala telescopes to undertake a search for emission in the 37.7 GHz class II methanol transition ($7_{-2} \rightarrow 8_{-1}E$) toward a total of 70 sources. Forty-six of these sources were observed with the ATNF Mopra 22 m telescope, and for these simultaneous observations of both the $6_2 \rightarrow 5_3A^-$ and $6_2 \rightarrow 5_3A^+$ (38.3 and 38.5 GHz, respectively) were also obtained. Of the 29 sources observed with the Onsala telescope at 37.7 GHz, separate observations of the 38.3 GHz transition were made toward 27 and of the 38.5 GHz transition toward 4. The position searched, rms noise level, and velocity range covered for the observed sources for all three transitions are given in Table 1.

Maser emission from the 37.7 GHz $7_{-2} \rightarrow 8_{-1}E$ transition was detected toward 13 sources. Quasi-thermal 37.7 GHz emission was detected toward Orion KL, which was observed as part of system testing. There are several reasons why we are confident that (with the exception of Orion KL) we are observing maser emission in these transitions, despite the peak flux density of some of the sources being <5 Jy. For about half the sources, the large peak flux density and narrow line width (<0.5 km s^{-1} in most cases) leave little doubt that this is maser emission. For the remaining sources the emission is also narrow and coincides in velocity with strong spectral features in other methanol maser transitions (see Section 3.1). The spectra of the detected maser sources are shown in Figures 1 and 2 and the properties of the emission are summarized in Table 2. Combining the results of the 37.7 GHz maser search of Haschick et al. (1989) with those reported here, a total of 77 class II methanol maser sites have been searched for the 37.7 GHz transition, resulting in a total of 13 detections of masers. Eight of the detections (all in the southern hemisphere) are reported here for the first time and this increases the number of sources which are known to show maser emission in this transition by more than a factor of two.

Maser emission from the $6_2 \rightarrow 5_3A^-$ and $6_2 \rightarrow 5_3A^+$ transitions (38.3 and 38.5 GHz, respectively) was detected toward three sources, one of which (G 345.010+1.792) is a new detection. The spectra of the 38.3 and 38.5 GHz masers are shown in Figure 3 and the properties of the emission are summarized in Tables 3 and 4.

3.1. Comments on Individual Sources of Interest

W3(OH) (G 133.94+1.04). This is the archetypal class II methanol and OH maser source. It is one of the five sources with detected maser emission at 37.7 GHz in the only previous publication studying this transition (Haschick et al. 1989). In a detailed study of class II methanol masers in W3(OH), Sutton et al. (2001) identified the 37.7 GHz emission as having an unusual profile compared to the other class II transitions and requested careful reobservation to confirm its nature. Our Onsala observations show a very similar spectrum to that observed by Haschick et al. (1989), although the peak flux density peak is somewhat weaker the velocities agree (once account is taken of the different rest frequencies). W3(OH) also shows emission from both the 38.3 and 38.5 GHz transitions. The peak intensity of the emission detected in the Onsala observations is similar to that observed by Haschick et al. (1989), as is the velocity of the narrow emission (we have not attempted to fit the "pedestal" component). The spectrum of these two transitions is similar to that seen in the $7_2 \rightarrow 6_3A^-$ and $7_2 \rightarrow 6_3A^+$ class II transitions

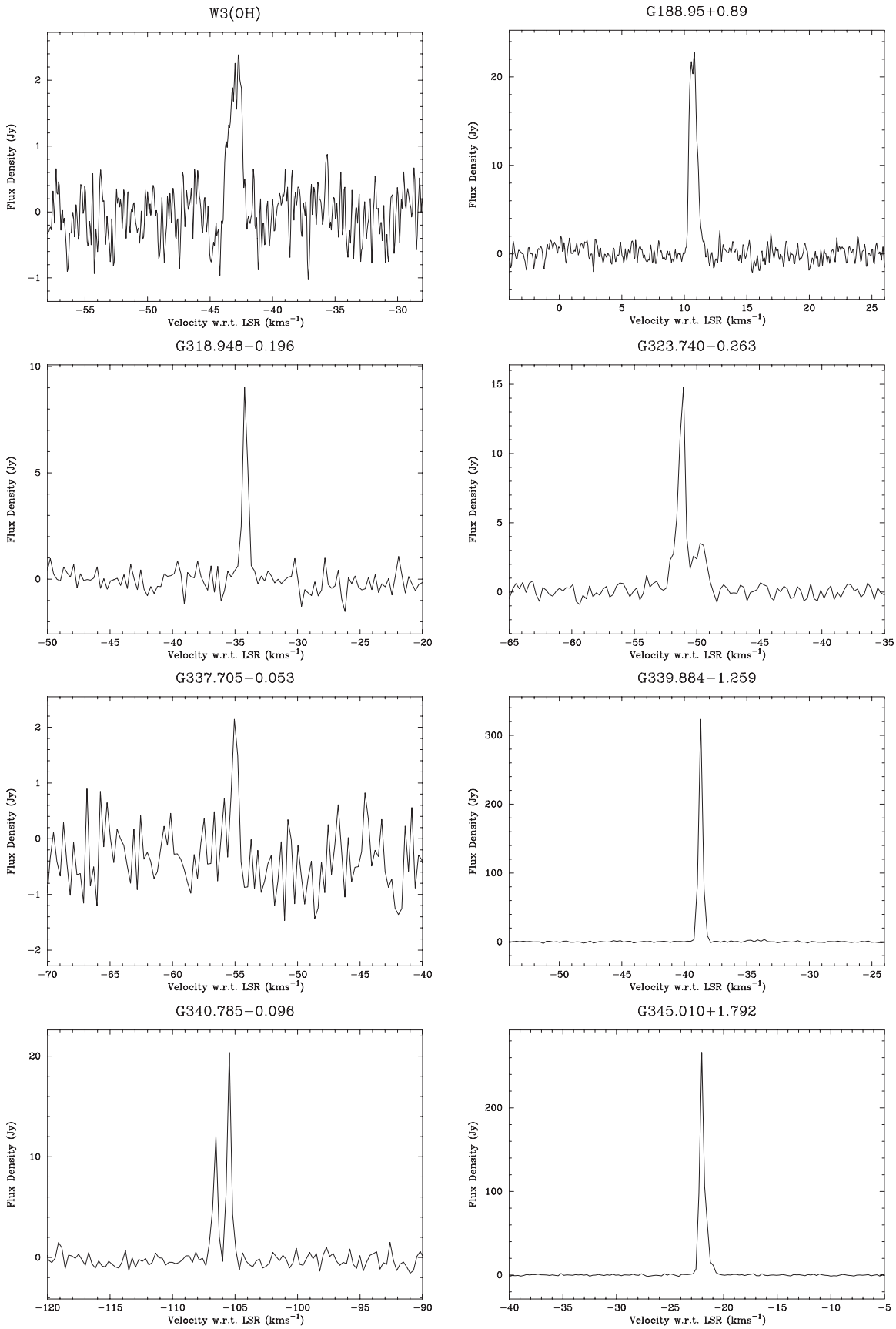

Figure 1. Spectra of masers detected in the 37.7 GHz transition.

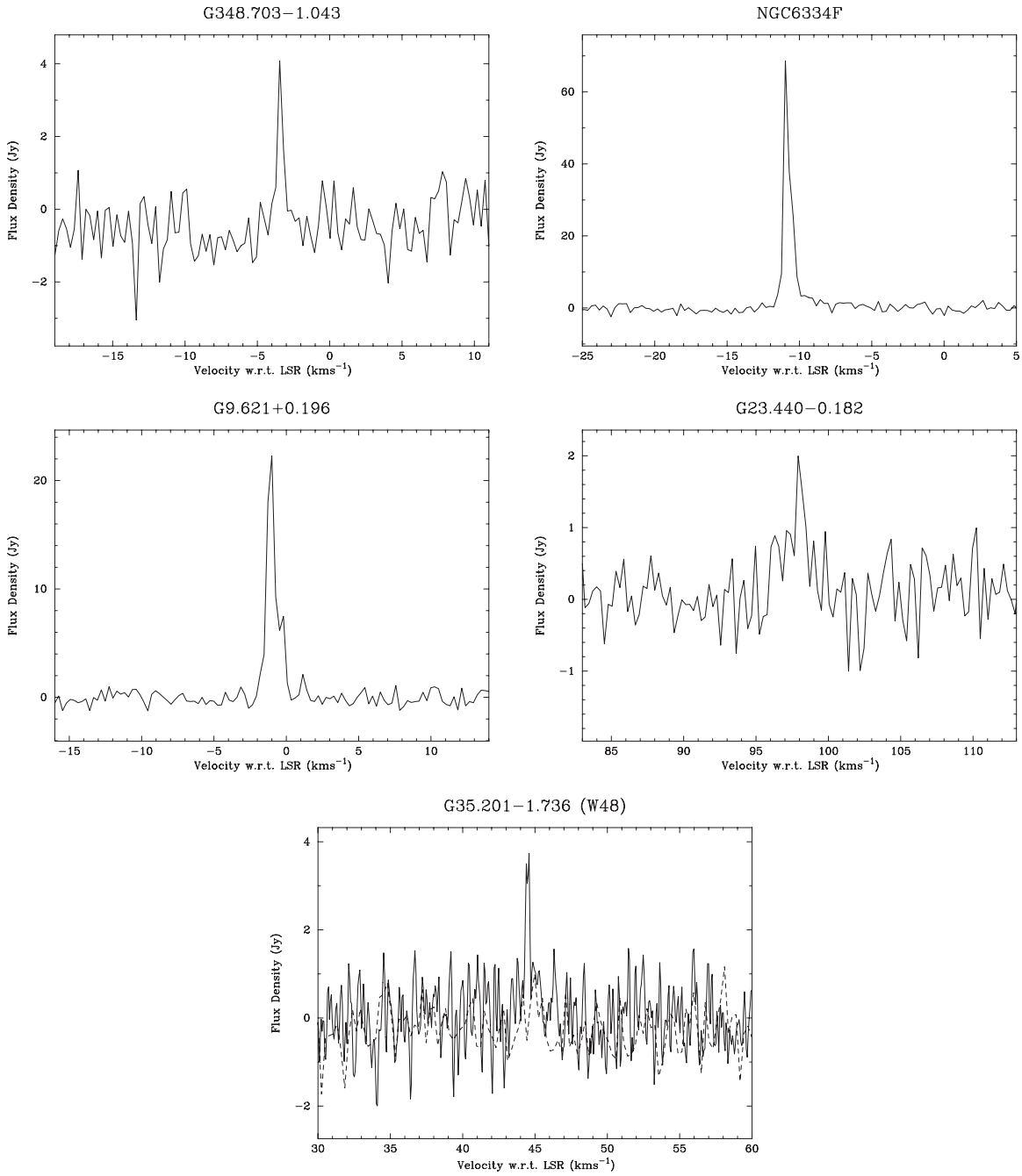

Figure 2. Spectra of masers detected in the 37.7 GHz transition (continued).

at 86.6 and 86.9 GHz (Sutton et al. 2001), which are in the same transition series. The 107 GHz masers also show a strong narrow peak at a velocity of −43.1 km s^{-1}. So in summary, the relatively weak maser emission first detected in these three transitions by Haschick et al. (1989) has changed little over the approximately 17 year interval between those observations and the ones reported here.

G 188.95+0.89. This source hosts a moderately strong 6.7 GHz methanol maser with a peak flux density of approximately 500 Jy at a velocity of 11 km s^{-1} (Caswell et al. 1995c). All of the other class II masers observed in this source also have their peak emission at velocities of around 10–11 km s^{-1}. The 37.7 GHz emission in this source was first detected by Haschick et al. (1989), who observed it to have a peak flux density of approximately 12 Jy. Our Onsala observations detect emission at the same velocity, with a peak flux density approximately a factor of two greater.

G 318.948–0.196. This is a moderate intensity 6.7 GHz methanol maser for which the peak emission in all the detected class II methanol maser transitions (6.7, 12.2, 37.7, and 107 GHz) is at around −34.5 km s^{-1} (Caswell et al. 1995c, 1995b, 2000), approximately the middle of the total velocity range of the 6.7 and 12.2 GHz emission.

G 323.740–0.263. This is a strong (∼3000 Jy) 6.7 GHz methanol maser. All of the observed class II methanol maser transitions in this source (including the newly detected 37.7 GHz maser) peak at velocities between −52 and −50 km s^{-1}.

G 337.705–0.053. This source was observed at 107 GHz by Caswell et al. (2000) who list it as possibly having weak 107 GHz methanol maser emission in the range −55 to

Table 2
Characteristics of the Sources Detected in the 37.7 GHz Methanol Transition

Source Name	Right Ascension (J2000)	Declination (J2000)	Peak Flux Density(Jy)	Velocity (km s^{-1})	Full Width at Half-maximum (km s^{-1})
W3(OH)	02:27:03.8	+61:52:25	2.2(0.2)	−42.96(0.03)	1.01(0.05)
G 188.95+0.89	06:08:53.7	+21:38:30	23.4(0.6)	10.74(0.01)	0.68(0.01)
G 318.948–0.196	15:00:55.4	−58:58:53	9.3(0.5)	−34.19(0.01)	0.47(0.03)
G 323.740–0.263	15:31:45.6	−56:30:50	14.6(0.5)	−51.18(0.01)	0.64 (0.02)
			3.7(0.4)	−49.7(0.05)	1.04 (0.12)
G 337.705–0.053	16:38:29.7	−47:00:35	2.4(0.6)	−55.00(0.06)	0.46 (0.14)
G 339.884–1.259	16:52:04.8	−46:08:34	323(0.9)	−38.70(0.001)	0.38 (0.001)
G 340.785–0.096	16:50:14.8	−44:42:25	20.5(0.7)	−105.48 (0.01)	0.38 (0.01)
			12.4(0.7)	−106.57 (0.01)	0.39 (0.03)
G 345.010–1.792	16:56:47.7	−40:14:26	207(1.0)	−22.10(−)	0.33(0.001)
			93.8(0.7)	−21.83(−)	0.72(0.006)
			11.0(1.1)	−20.90(−)	0.26(0.03)
G 348.703–1.043	17:20:04.1	−38:58:30	4.4(0.9)	−3.40(−)	0.36(0.08)
NGC 6334F	17:20:53.4	−35:47:00	70.4(1.5)	−10.91(0.01)	0.36(0.01)
			21.9(1.2)	−10.45(0.02)	0.4(-)
			3.5(0.6)	−10.1(0.2)	2.9(0.4)
G 9.621+0.196	18:06:14.8	−20:31:32	23.6(0.6)	−1.08(0.01)	0.59(0.01)
			8.3(0.7)	−0.28(0.02)	0.43(0.05)
G 23.440–0.182	18:34:39.2	−08:31:24	2.3(0.3)	98.03(0.04)	0.5(-)
G 35.201–1.736	19:01:45.5	+01:13:29	3.2(1.3)	44.51(0.03)	0.53(0.2)

Notes. For parameters where the error is indicated by a dash that particular parameter was held fixed in the Gaussian fit.

Table 3
Characteristics of the Sources Detected in the 38.3 GHz Methanol Transition

Source Name	Right Ascension (J2000)	Declination (J2000)	Peak Flux Density(Jy)	Velocity (km s^{-1})	Full Width at Half-maximum (km s^{-1})
W3(OH)	02:27:03.8	+61:52:25	10.9(0.4)	−43.09(0.008)	0.91(0.03)
G 345.010–1.792	16:56:47.7	−40:14:26	9.4(0.7)	−22.30(0.02)	0.46(0.05)
			7.6(0.6)	−21.38(0.03)	0.61(0.07)
NGC 6334F	17:20:53.4	−35:47:00	174(7.0)	−10.49(0.001)	0.34(0.02)
			32.9(2.7)	−11.02(0.008)	0.38(0.04)

Notes. For parameters where the error is indicated by a dash that particular parameter was held fixed in the Gaussian fit.

Table 4
Characteristics of the Sources Detected in the 38.5 GHz Methanol Transition

Source Name	Right Ascension (J2000)	Declination (J2000)	Peak Flux Density(Jy)	Velocity (km s^{-1})	Full Width at Half-maximum (km s^{-1})
W3(OH)	02:27:03.8	+61:52:25	16.1(1.1)	−42.88(0.009)	0.47(0.03)
G 345.010–1.792	16:56:47.7	−40:14:26	5.0(0.5)	−22.25(0.06)	1.04(0.15)
			3.6(0.8)	−21.26(0.05)	0.48(0.13)
NGC 6334F	17:20:53.4	−35:47:00	150(20)	−10.47(0.06)	0.33(0.11)
			44(15)	−10.94(0.11)	0.37(0.09)

Notes. For parameters where the error is indicated by a dash that particular parameter was held fixed in the Gaussian fit.

−50 km s^{-1} because of a deviation in the thermal profile over this velocity range compared to that seen in the 156.6 GHz transition. The 6.7 and 12.2 GHz methanol masers in this source have their peak at a velocity of −54.6 km s^{-1} (Caswell et al. 2011; Breen et al. 2011b), similar to the observed 37.7 GHz emission peak at −55 km s^{-1}. The detection of a 37.7 GHz maser in this source strengths the likelihood that the tentative 107 GHz maser detection is real (see Section 4.2).

G 339.884–1.259. This is one of the strongest 6.7 GHz methanol maser sources and has been detected in a number of the weaker class II maser transitions including 107 GHz (Val'tts et al. 1999; Caswell et al. 2000) and 19.9 GHz (Ellingsen et al. 2004), and now in the 37.7 GHz transition. All of these transitions with the exception of the 19.9 GHz peak at a velocity of −38.7 km s^{-1}. The 37.7 GHz emission has a peak flux density of approximately 320 Jy, making it the strongest known source in this transition.

G 340.785–0.096. This source has been previously detected in the 6.7, 12.2, and 107 GHz transitions. The strongest emission is most often at a velocity of around −105 km s^{-1} (the velocity

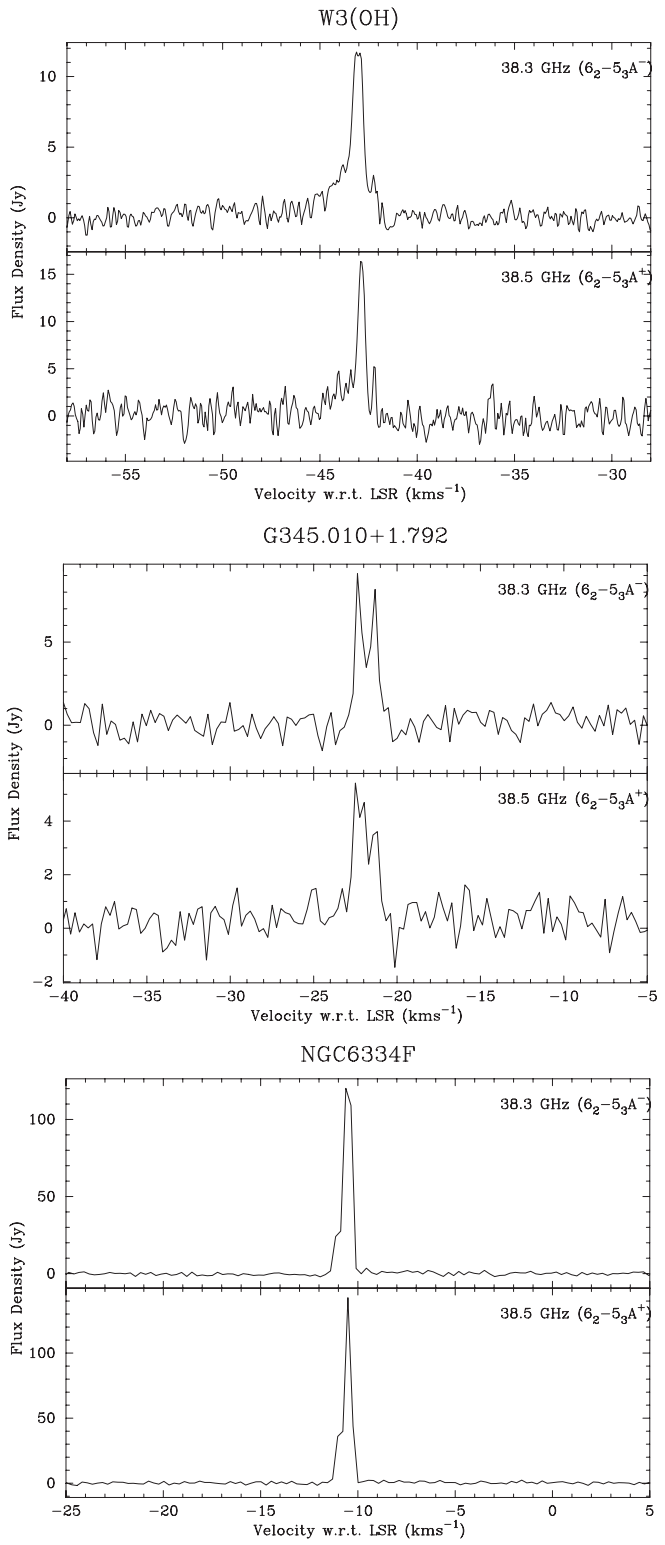

Figure 3. Spectra of masers detected in the 38.3 and 38.5 GHz transitions.

of the 37.7 GHz peak), although the most recent 6.7 GHz observations of Caswell et al. (2011) find the strongest 6.7 GHz emission at −108.1 km s^{-1}.

G 345.010+1.792. This source holds the record for the largest number of class II methanol maser transitions observed toward any one source (see, for example, Cragg et al. 2001). Observations of this source have been made in all but one of the known class II methanol maser transitions, the exception being the 29.0 GHz transition (for which the only published search is by Wilson et al. 1993). Maser emission has been detected in all of these transitions, except for the 23.1 GHz transition which was not detected in the sensitive search of Cragg et al. (2004). The observations undertaken here are the first toward this source in the 37.7, 38.3, and 38.5 GHz transitions, all of which are detected. The 37.7 GHz maser in this source has a peak flux density in excess of 250 Jy (it is the second strongest source in this transition) and it is the only new detection in the 38.3 and 38.5 GHz transitions. Early observations of this source at 6.7 GHz in 1992 (e.g., Caswell et al. 1995c) showed the peak at around −17 km s^{-1}, but in more recent observations (Ellingsen et al. 2004; Caswell et al. 2010) that feature has declined and the strongest feature is at −21 km s^{-1}, very close to the velocity of the peak emission in the 12.2, 37.7, 38.3, 38.5, and 107 GHz transitions. The 38.3 and 38.5 GHz spectra clearly show that there are at least two spectral features at velocities around −22 to −21 km s^{-1}, which helps to explain some of the difficulty encountered by Cragg et al. (2001) simultaneously modeling all the methanol transitions in this region with a single component. Interestingly, the 19.9 GHz peak is at −17.6 km s^{-1} (the velocity of the old 6.7 GHz peak), and there is also 12.2 GHz emission and weak 107 GHz maser at the same velocity. However, there is no 37.7, 38.3, or 38.5 GHz emission near −17.6 km s^{-1} at the sensitivity of these observations.

G 348.703–1.043. The peak of the methanol masers at 6.7, 12.2, 107, and the newly detected 37.7 GHz maser all lie at a velocity of approximately −3.5 km s^{-1}. At 6.7 GHz this source has a velocity range of −17.5 to −2.5 km s^{-1} (Caswell et al. 2010), which places the peak near the redshifted extreme.

NGC 6334F (G 351.416+0.645). This is a very well-studied southern star formation region, which shares many characteristics with the W3(OH) region. Like W3(OH), it shows emission in a very large number of class II methanol maser transitions (Cragg et al. 2001) and was one of the sources detected in the 37.7, 38.3, and 38.5 GHz search of Haschick et al. (1989). There are in fact two sites of strong (>1000 Jy peak flux density) 6.7 and 12.2 GHz methanol masers separated by around 2″ with overlapping velocity ranges. One of the sites is projected against the strong cometary ultracompact (UC) H II region and has its peak 6.7 GHz emission at −10.4 km s^{-1} (Caswell et al. 2010), while the other is offset (Ellingsen et al. 1996; Caswell 1997) from the radio continuum and has its 6.7 GHz peak emission at −11.1 km s^{-1}. These two sites are far too close to distinguish in the present observations and interferometry will be required to determine if the 37.7 and 38 GHz masers are associated with both regions or just one. However, for each of the three transitions Gaussian fitting (Tables 2–4) shows one spectral peak at a velocity of around −10.4 km s^{-1} and a second at a velocity around −11 km s^{-1}. The 38 GHz transitions being strongest at the former and the 37.7 GHz being strongest at the latter. NGC 6334F is the only source which shows strong emission (>20 Jy) in all of these three transitions.

In 1989 the 37.7 GHz emission in this source had a peak flux density of approximately 100 Jy at a velocity of −11 km s^{-1} (after adjusting the velocity to the same rest frequency used here). In the intervening 20 years the peak of the 37.7 GHz emission has declined by approximately 30%. The velocity of the peak emission at 38.3 and 38.5 GHz also agrees to within 0.1 km s^{-1} with that observed by Haschick et al. (1989), but while the 38.3 GHz emission is significantly weaker (a peak of 120 Jy, compared to 330 Jy in 1988), the 38.5 GHz emission has approximately the same intensity.

G 9.621+0.196. This is the strongest 6.7 GHz class II methanol maser, with a peak flux density in excess of 5000 Jy, and it is also distinguished in being the best studied of the "periodic" methanol masers (Goedhart et al. 2003, 2005; Vlemmings et al. 2009). The 6.7 and 12.2 GHz emission in this source peaks at a velocity of around 1.3 km s^{-1}, but the 37.7 GHz masers are offset from this by more than 2 km s^{-1}, and peak at −1.1 km s^{-1}. The 37.7 GHz spectrum suggests that there might be weak (2 Jy) emission at the peak velocity of the stronger masers, but more sensitive observations are required to confirm this. Previous observations of the 37.7 GHz methanol masers in this source (Haschick et al. 1989) observed slightly stronger peak flux density (30 Jy), but at the same velocity (−1.0 km s^{-1} after correcting for the different rest frequency). The peak in the 107 GHz spectrum is at −0.5 km s^{-1} (Caswell et al. 2000), so it is also blueshifted with respect to the lower frequency transition, although less so than the 37.7 GHz emission. The velocity of the 107 GHz peak may be affected by blending with the broad thermal emission in this source, which future higher spatial resolution observations may be able to resolve. There is a 10 Jy 107 GHz peak approximately coincident in velocity with the 6.7 and 12.2 GHz peaks. This is also one of only five sources which show maser emission from the 85.5 GHz $6_{-2} \rightarrow 7_{-1}E$ (which is in the same transition series as the 37.7 GHz transition), and this has its peak velocity at −0.9 km s^{-1} (Cragg et al. 2001). The 37.7 GHz peak corresponds to emission which has a peak flux density of about 20 Jy at 12.2 GHz and 80 Jy at 6.7 GHz (Caswell et al. 2010; Breen et al. 2011b).

G 23.440–0.182. This source shows class II methanol maser emission over a velocity range from 94 to 113 km s^{-1} (Caswell et al. 1995c). The strongest 6.7 GHz emission is at velocities around 103 km s^{-1}, and strong 12.2 GHz emission has been seen at similar velocities. The 107 and 37.7 GHz masers in this source both have peak velocities much closer to the blueshifted end of the spectrum, at 97.2 and 98 km s^{-1}, respectively (Caswell et al. 2000). At both 6.7 and 12.2 GHz there are a number of secondary spectra features in this velocity range, which are much more stable than the spectral features at velocities greater than 100 km s^{-1} (Caswell et al. 1995a).

G 35.201–1.736 (W48). This well-studied star formation region is one of the original 37.7 GHz maser detections of Haschick et al. (1989), who observed emission with a peak flux density of approximately 20 Jy toward this source. Observations with Onsala in late 2005 detected a much lower peak flux density of 3.2 Jy, while the observations made four years later with Mopra detected no 37.7 GHz emission from this source stronger than 1.5 Jy. Further observations were undertaken with Mopra in 2011 February to check this result and also failed to detect any 37.7 GHz emission with a 3σ limit of 1.1 Jy. So in a period of 20 years the 37.7 GHz emission in this source has faded by a factor of more than 10. The 12.2 GHz emission in this source peaks at a velocity of 44.6 km s^{-1} (the velocity of the 37.7 GHz peak), while the 6.7 and 107 GHz emission peaks at a lower velocity of 42 km s^{-1}.

3.2. Comparison of 37.7 and 6.7 GHz Masers

Figures 1–3 show that the spectra of the 37.7 (and 38 GHz) masers are much simpler than their 6.7 GHz counterparts and typically consist of one or two spectral features. For the majority of sources the 37.7 GHz peak coincides in velocity with the 6.7 GHz maser peak to within 0.2 km s^{-1}, and where it does not, it is always coincident with a secondary peak in the 6.7 GHz spectrum (G 9.621+0.196 is a notable example). It is clear that all of the brightest 6.7 GHz masers have an associated 37.7 GHz maser, but the relative intensity of that emission varies significantly, from a few Jy to several hundred Jy. Also, there are a number of relatively weak (<100 Jy peak flux density) 6.7 GHz methanol masers which have an associated 37.7 GHz maser. The 37.7 GHz masers have velocity ranges of at most a few km s^{-1}, compared to typical ranges of ∼10 km s^{-1} for the 6.7 GHz methanol masers they are associated with.

In any search for rare, weak masers it is important to consider the role the sensitivity limit may have on the results. Breen et al. (2011b) have investigated this issue in some detail for their search for 12.2 GHz methanol masers toward the methanol multibeam (MMB) sample and much of the discussion in their Sections 5.2 and 5.3 is relevant to this search. They identify several lines of evidence that suggest that sensitivity is not the limiting factor and here we summarize the relevant ones. In most strong 6.7 GHz masers there are multiple secondary features with flux densities within a factor of a few of the peak intensity. The sensitivity of our observations is such that were there 37.7 GHz emission associated with these secondary peaks we would detect it, unless the 6.7:37.7 GHz flux density ratio were always much lower for the secondary features than the main peak. This seems unlikely given that the ratio of 6.7:12.2 GHz features within a single source shows much less scatter than in the population as a whole (Breen et al. 2011b). These observations are consistent with the hypothesis that the total volume of gas conducive to 37.7 GHz maser emission is significantly smaller than that for the 6.7 GHz emission. Additional evidence that sensitivity is not the primary factor in determining the number of 37.7 GHz masers we have detected in our search comes from Section 4.2, where we show that the 37.7 GHz masers are preferentially associated with the most luminous 6.7 GHz masers, whereas our sample contains sources with a broad range of 6.7 GHz maser luminosities

4. DISCUSSION

The search which we have undertaken here can be directly compared to the search for the $6_{-2} \rightarrow 7_{-1}E$ (85.5 GHz) and $7_2 \rightarrow 6_3A^-$ (86.6 GHz) methanol maser transitions undertaken by Ellingsen et al. (2003). The 37.7 GHz masers are from the same transition family as the 85.5 GHz, and the 38.3 GHz masers are from the same transition family as the 86.6 GHz. The lower frequency class II masers in each transition family are typically stronger, so we would expect to detect all of the 85.5 and 86.6 GHz maser sources, in addition to some sources not seen in those transitions. Broadly speaking those expectations are only partially met. A total of 45 sites have been searched for 85.5 GHz methanol masers resulting in the detection of five sources (Cragg et al. 2001; Sutton et al. 2001; Minier & Booth 2002; Ellingsen et al. 2003)—specifically G 328.808+0.633, G 345.010+1.792, G 9.621+0.196, G 29.95–0.02, and DR21(OH). These have all been observed at 37.7 GHz by us; two of these resulted in 37.7 GHz detections with a peak flux density around 20 times greater than that observed at 85.5 GHz. However, for G 328.808+0.633, G 29.95–0.02, and DR21(OH), no 37.7 GHz emission was detected and we are able to place an upper limit of ∼1 on the 37.7:85.5 GHz peak flux density ratio. Looking at the converse cases where we have a 37.7 GHz maser with no associated 85.5 GHz maser we can set a lower limit on the 37.7:85.5 GHz peak flux ratio in those sources and these values range from <1 through to approximately 300 for G 339.884–1.259. So the range of observed ratios spans at least

2.5 orders of magnitude, which is comparable to that observed for the 6.7:12.2 GHz peak flux density ratio (Breen et al. 2010).

The correspondence between the 38.3/38.5 GHz ($6_2 \rightarrow 5_3A^-/A^+$) and the 86.6/86.9 GHz ($7_2 \rightarrow 6_3A^-/A^+$) transitions appears generally closer, but this could be the result of small number statistics. Two of the three 38.3/38.5 GHz sources also have associated 86.6/86.9 GHz maser emission (W3(OH) and G 345.101+1.792), and in both of these cases the 38 GHz masers are approximately a factor of two stronger than the 86 GHz masers. The exception is NGC 6334F, which has strong (>100 Jy peak) 38 GHz masers, but no detected 86 GHz masers at a sensitivity of a few Jy.

4.1. Comparison of Different Class II Methanol Transitions

Combining the results presented here with data from the literature we are now in a position to compare the characteristics of a dozen different class II methanol maser transitions in a sample of 25 sources. These dozen transitions constitute all the published class II methanol maser transitions with the exception of the 29.0 GHz $8_2 \rightarrow 9_1A^-$ (Wilson et al. 1993) and the 157 GHz $J_0 \rightarrow J_{-1}E$ series (Slysh et al. 1995). The 25 sources represent the complete sample of currently known 107 GHz methanol masers. The data are collated in Table 5 and are approximately 95% complete for these transitions (the least complete transition is the 108.8 GHz observations). The comparison of the emission from the different transitions has been made at the velocity of the 37.7 GHz peak, or where there was no emission in that transition detected, at the velocity of the 107 GHz peak. This table shows that 37.7 GHz is the fourth most common class II methanol maser transition, having been detected toward approximately half of the sample, with many of the detections having peak flux density in excess of 10 Jy.

At the bottom of the table we have attempted to summarize some of the key characteristics of the 12 transitions for which moderately large searches have been made. Some of the numbers are a little uncertain; for example, the exact number of 6.7 GHz methanol masers which have been detected keeps increasing as the results of the MMB survey (and other searches) are published, and determining exactly how many class II sources have been searched for a particular transition is complicated by inconsistencies in naming sources and similar issues. However, these minor uncertainties are insufficient to obscure the general trends displayed by the different transitions. It is clear from Table 5 that the population of 6.7 and 12.2 GHz transitions differs significantly from the other class II methanol maser transitions. The 6.7 GHz transition is the only one for which any significant unbiased searches have been undertaken and extrapolating the results from the MMB suggests that the total Galactic population exceeds 1000 sources. A sensitive follow-up toward all the MMB detections south of declination -20° detected 12.2 GHz masers toward 43% of 6.7 GHz methanol masers (Breen et al. 2011a). For the remaining transitions, generally of order 50 class II maser sites have been searched, typically with a strong bias toward those with strong 6.7 GHz methanol masers. Given this bias, the tabulated detection percentages for these remaining transitions are likely to be upper limits on the detection percentage taken over the entire population of all class II maser sites. Aside from the 6.7 and 12.2 GHz methanol masers, it is clear that the other class II transitions are much rarer (detected toward < 5% of the 6.7 GHz population), and where they are detected, the emission is almost always weaker than the 6.7 GHz peak emission in all other transitions. Hereafter, we use the term strong, common methanol masers to refer to the 6.7 and 12.2 GHz transitions and rare, weak to refer to the other class II methanol maser transitions.

Looking at the results summarized in Table 5 the only common pattern which can be seen is that many of the sources (9 out of 25) only show emission at 6.7, 12.2, and 107 GHz. More generally, two-thirds of the sample exhibits class II methanol maser emission in at least one other transition. However, beyond a propensity for some transitions to be more common than others, many different combinations of rare, weak transitions are observed. Where the rare, weak transitions are observed they are often at the same velocity as the strongest 6.7 and 12.2 GHz emission, although in some sources (e.g., G 9.621+0.196), this is not the case. Also, several of the 19.9 GHz class II masers (G 339.884–1.259 and G 345.010+1.792) peak at velocities significantly offset from the strongest emission in other transitions suggesting that this transition in some cases favors different conditions from those which give rise to the presence of the rare, weak masers in most sources.

4.2. A Maser-based Evolutionary Timeline

Assuming that all Galactic high-mass star formation regions show maser emission during their evolution, the presence and absence of different maser transitions toward specific regions can potentially be used to trace the changes in physical conditions and hence their evolutionary state. While this is not a new idea (see, for example, Lo et al. 1975; Genzel & Downes 1977), it requires large, sensitive, high-resolution, preferably unbiased samples of a variety of maser transitions which are only now becoming available. Combining data from existing unbiased OH maser searches (Caswell 1998) with the recently released MMB survey (Caswell et al. 2010; Green et al. 2010; Caswell et al. 2011), the HOPS 22 GHz water maser survey (Walsh et al. 2011) and complementary data at other wavelengths (e.g., the *Spitzer* GLIMPSE Legacy survey and the submillimeter ATLASGAL survey) it is becoming feasible to make statistical studies of the properties of high-mass star formation regions associated with masers. A qualitative maser-based evolutionary timeline involving all the strong, common maser transitions observed in high-mass star formation regions was first proposed by Ellingsen et al. (2007) and has recently been improved and quantified by Breen et al. (2010). High-mass star formation occurs predominantly in clusters, where there are often observed to be objects at a range of evolutionary stages within close proximity (e.g., Wang et al. 2011). However, class II methanol masers are confined to small volumes, close to a particular young stellar object within the cluster, so we expect the maser evolutionary timeline to reflect the properties of an individual object, rather than the cluster as a whole. This is supported by the results of Breen et al. which show that the masers are more sensitive probes of changes in physical condition (and hence evolutionary state) than properties such as the mid-infrared colors, which reflect the properties of the bulk emission of warm dust. Furthermore, where multiple class II maser transitions are observed toward the same region observations to date show that they are always coincident on arcsecond scales. This means that although interferometric observations are required to establish the coincidence definitively, we are confident that it is reasonable to use our observations with spatial resolutions of $1'$–$2'$ and assume that the emission from the various transitions is associated with the same individual object within the cluster environment.

Table 5

The Flux Density at the Velocity of the Peak in the 37.7 GHz Transition, (or the 107.0 GHz Transition for Sources with no 37.7 GHz Emission) of the 6.7, 12.2, 19.9, 23.1, 37.7, 38.3, 38.5 85.5, 86.6, 107.0, 108.8, and 156.6 GHz Methanol Transitions Toward All Star Formation Regions with Known 107.0 GHz Methanol Masers

Source	Velocity ($km\ s^{-1}$)	Flux Density												References
		6.7 GHz (Jy)	12.2 GHz (Jy)	19.9 GHz (Jy)	23.1 GHz (Jy)	37.7 GHz (Jy)	38.3 GHz (Jy)	38.5 GHz (Jy)	85.5 GHz (Jy)	86.6 GHz (Jy)	107.0 GHz (Jy)	108.8 GHz (Jy)	156.6 GHz (Jy)	
W3(OH)	−43.0	3000	600	44.3	9.5	2.2	11.0	16.0	<0.7	6.7	72	<0.6	<9	16,18,19,23,24
G 188.946+0.886	10.9	495	235	<0.20		23.4	<1.8	<3.3	<2.1	<0.8	15.5	<4.8	<2	4,5,6,9,11,12,22
G 192.600–0.048	4.2	72	<0.4[†]	<0.19		<2.4	<2.1		<1.8	<2.2	5.8	<4.5	<3	2,4,6,11,12,22
G 310.144+0.760	−56	130	114	<0.16	<0.8	<1.2	<1.2	<1.2	<1.4	<2.1	23		<3	6,10,11,12
G 318.948–0.196	−34.2	780	180	<0.17	<0.8	9.3	<1.5	<1.2	<2.0	<2.2	5.7	<3*	2.4	4,5,6,10,11,12,22
G 323.740–0.263	−51.2	132	135	0.15	<0.9	14.6	<1.2	<1.2	<1.8	<1.9	9.5	<5.4	<4*	6,10,11,12,22
G 327.120+0.511	−89.8	25	5	<0.17	<0.9	<1.2	<1.2	<1.2	<1.5	<2.2	9.2		<2.8	4,5,6,10,11,12
G 328.808+0.633	−43.5	315	5	0.8	<1.0	<1.5	<1.5	<1.5	1.6	<2.4	5.5	<6*	<8*	6,9,10,11,12,22
G 336.018–0.827	−40.2	30	7.7	<0.21	<0.8	<1.8	<1.8	<1.8	<1.3	<2.7	6	<5.7	<5*	3,6,8,9,10,11,12,22
G 339.884–1.259	−38.7	1520	846	<0.2[†]	<0.6	323	<2.4	<2.4	<1.1	<1.7	64	<5.4	4	3,6,8,9,10,11,12,22
G 340.054–0.244	−62.8	1.5	<0.3[†]	<0.20	<0.8	<1.8	< 2.1	<1.8		<2.3	2.9		<2	3,6,8,10,11,12
G 340.785–0.096	−105.5	120	42	<0.76	<0.7	20.5	<2.1	<1.8	<1.8	<1.9	6.1		<2	3,6,8,10,11,12
G 345.003–0.223	−26.9	102	<0.5[†]	0.47	<0.6	<2.1	<2.1	<2.1	<2.0	<2.9	3.5	<1.5*	<6*	3,6,7,9,10,7,22
G 345.010+1.792	−22.1	200	200	<0.2[†]	<0.5	207	9.4	5.0	10.0	2.8	4.1	82	18	3,6,7,9,10,11,12,22
G 345.504+0.348	−17.7	300	8.4	<0.65	<0.8	<2.1	<2.1	<2.1	<4.7	<2.4	2.3	<2*	<4*	3,6,7,10,11,12
G 348.703–1.043	−3.3	65	34	<0.39	<0.9	4.4	<2.1	<2.1	<1.5	<2.7	7.6		<1.5	3,6,7,10,11,12
NGC 6334F	−11.1	1840	692	30	4	70.4	32.9	44	<2.5*	<1.0*	10		<17*	3,6,7,9,10,7,12,22
G 353.410–0.360	−20.5	116	21	0.33	<0.8	<1.8	<1.8	<1.8	<2.1	<2.0	4.5		<2	3,6,7,10,11,12
G 9.621+0.196	−1.1	80	20	<0.22	<0.6	23.6	<1.8	<1.8	1.2	<2.3	22	<3*	<3*	3,6,9,10,11,12,13
G 12.909–0.260	39.5	269	11.5	<0.27	<0.8	<1.2	<1.2	<1.2	<3.8	<8.6	5.5	<3*	<3*	5,6,9,10,11,12,13,22
G 23.010–0.411	75.9	405	28	<0.26	<0.9	<0.9	<0.9	<0.9	<3.8		5.2	<5.1	<2	4,5,6,9,10,12,22
G 23.440–0.182	98.0	23	9	<0.24	<0.9	2.3	<1.2	<1.2	<4.0*	<4.1	4		<2	4,5,6,10,11,12
G 35.201–1.736	44.5	260	109	<0.51	<0.9	3.2	<1.5	<1.5	<1.1	<2.3	22	<4.8	4.6	4,5,6,9,10,11,12
Cep A	−2.2	1420	<7[†]			<2.1	<1.5		<5.0	<5.0	16	<5.0	<3	14,15,16,17,18
NGC 7538	−59.0	15	<5[†]	0.21	0.21	<2.1	<1.8		<5.0	<5.0	10.1	<4.0*		1,17,20,21,23,24
Det. in Sample of 25		25	20(24)	5(7)	3	12	3	3	3	2	25	1	4	
Class II searched		>800	>600	∼29	∼75	∼79	∼76	∼60	∼45	∼32	∼175	∼45	∼67	
Detected /%		>800/100	>260/43	7/24	3/4	13/16	3/4	3/5	5/11	3/9	25/14	2/4	4/6	
Median peak flux (Jy)		300	75.5	0.47	4	17.6	11	16	1.6	4.75	6.1	82	4.3	

Notes. The 37.7, 38.3, and 38.5 GHz data are taken from this work. The rest of the information has been taken from the literature references given in the last column. Where upper limits are quoted they are three times the rms noise level in the spectra. Transitions where there is maser emission, but none at a velocity corresponding to the 37.7 GHz peak, are indicated with a, [†]. Transitions where thermal emission is detected are indicated with a * and the upper limited listed is 50% of the flux density of the thermal emission at the listed velocity. The total number of detections in each transition is tabulated at the bottom of the table, the numbers in brackets give the total number of detections from that transition at all velocities, not just the single velocity for each source listed in the table. The number of sources detected (given in the second last line) refers to all maser detections, not just those from the sample of 25 sources presented here and the percentage detection is with respect to the number of class II methanol maser positions searched. The median flux density refers only to the sample of 25 107 GHz methanol masers.

References. (1) Batrla et al. 1987; (2) Breen et al. 2010; (3) Breen et al. 2011b; (4) Caswell et al. 1995a; (5) Caswell et al. 1995b; (6) Caswell et al. 2000; (7) Caswell et al. 2010; (8) Caswell et al. 2011; (9) Cragg et al. 2001; (10) Cragg et al. 2004; (11) Ellingsen et al. 2003; (12) Ellingsen et al. 2004; (13) Green et al. 2010; (14) Koo et al. 1988; (15) Mehringer et al. 1997; (16) Menten 1991; (17) Minier & Booth 2002; (18) Slysh et al. 1995; (19) Sutton et al. 2001; (20) Szymczak et al. 2000; (21) Val'tts et al. 1995; (22) Val'tts et al. 1999; (23) Wilson et al. 1984; (24) Wilson et al. 1985.

Breen et al. find that the luminosity of the 6.7 and 12.2 GHz class II methanol masers is largest for the most evolved regions. This is consistent with theoretical models which predict that the luminosity will increase as the gas temperature increases, the density decreases and emission from the UC H II region increases (with the maser luminosity expected to catastrophically drop at some point, as discussed below). The rare, weak class II methanol maser transitions are typically found toward the brightest 6.7 GHz methanol masers and so studies of these transitions toward a larger sample of sources can potentially shed light on relatively short-lived phases during the evolution of high-mass star formation regions. It is well established that 6.7 GHz masers trace an evolutionary phase which largely precedes the formation of a UC H II region (Walsh et al. 2003; Minier et al. 2005; Ellingsen 2006). The exact mass range of the objects with an associated 6.7 GHz methanol maser is not well established, but it is known that class II methanol masers are not associated with low-mass stars (Minier et al. 2003; Xu et al. 2008). Ellingsen et al. (2004) investigated the radio continuum emission and OH masers associated with the 25 known 107 GHz methanol masers (see their Table 3) and found 50% show centimeter radio continuum emission stronger than a few mJy, while all but one have an associated main-line OH maser (the exception is G 192.600–0.048), and 50% have an associated OH satellite or excited-state maser. The presence of centimeter radio continuum and/or an OH maser (particularly an excited-state OH maser) strongly suggests a relatively evolved 6.7 GHz methanol maser region and so it appears that the 107 GHz methanol maser phase likely traces a late part of the class II methanol maser phase in star formation regions.

Breen et al. (2011a) have shown that there is a correlation between the integrated luminosity of the 6.7 and 12.2 GHz methanol masers and Breen et al. (2010) showed a similar correlation using the peak luminosity. Using the data summarized in Table 5 we investigated the relationship between the peak luminosities of various methanol maser transitions, but found that in all cases the correlation is weaker than that observed for the 6.7 and 12.2 GHz emission. Figure 4 shows the luminosity of the peak 12.2 GHz methanol maser emission versus the luminosity of the peak 6.7 GHz methanol maser emission for several different samples of sources. The black dots combine the 6.7 GHz data from the MMB and the 12.2 GHz survey of Breen et al. (2011a) and represent all 12.2 GHz maser detections south of declination −20°. We have in all cases used the best available estimate of the distance to calculate the luminosity, including parallax distances from Reid et al. (2009) and Rygl et al. (2010), H I self-absorption distances from Green & McClure-Griffiths (2011) and where neither of these was available we have used the near kinematic distance calculated using the method of Reid et al. (2009). In total, parallax or H I self-absorption distances were available for 84% of the 107 GHz sample and 68% of the comparison sample. Figure 4 demonstrates the well-established tendency for the peak of the 12.2 GHz emission to be weaker than the 6.7 GHz emission (although with several orders of magnitude scatter in the observed ratio), and we have plotted the same luminosity range on each axis so that the relationship can clearly be seen. The red triangles and purple squares are the 25 known 107 GHz methanol masers detected in the surveys of Val'tts et al. (1995) and Caswell et al. (2000) which are summarized in Table 5, with the purple squares represent the 37.7 GHz masers detected in this work (all of which have an associated 107 GHz methanol maser; although see the individual comments for G 337.705–0.053 for clarification for this source). These sources are largely (but not completely) a subset of the 12.2 GHz maser detections south of declination −20° and for these we use either the red circle or purple square symbols (rather than a black dot). Figure 4 shows that with one exception (interestingly G 192.600–0.048 again), all the 107 GHz methanol masers have a 6.7 GHz peak luminosity $\gtrsim$1000 Jy kpc^2, which represents only a small fraction (∼15%) of the class II methanol maser population as a whole. The largest and most sensitive search for 107 GHz methanol masers was undertaken by Caswell et al. (2000) and their sample of 84 sources deliberately included sources covering a wide range of 6.7 and 12.2 GHz peak flux densities. This means that the observed preference for 107 GHz methanol masers to be observed toward only the most luminous 6.7 GHz masers cannot be ascribed solely to selection bias (although a far greater fraction of the luminous sources have been searched for 107 GHz than the less luminous ones).

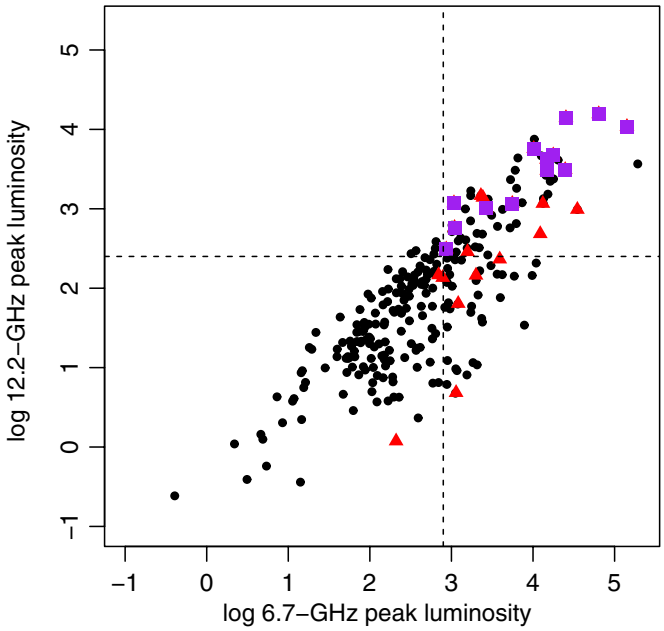

Figure 4. Luminosity of the 12.2 GHz maser peak vs. the luminosity of the 6.7 GHz maser peak for various maser samples. The red triangles represent sources with an associated 107 GHz methanol maser (but no 37.7 GHz maser) and the purple squares represent sources with associated 37.7 GHz methanol masers (all of which also have an associated 107 GHz maser). The black dots represent the 237 12.2 GHz methanol masers at declinations <−20°, from the survey of Breen et al. (2011a), The calculated luminosities assume isotropic emission and are in units of Jy kpc^2. For the distances used in the luminosity calculations we have used parallax measurements and H I self-absorption where available and assumed the near kinematic distance for the remaining sources. The vertical dashed line at 2.9 approximates the observed cutoff for the presence of 107 GHz masers (red triangles and purple squares), with the horizontal line at 2.4 showing the region containing all the 37.7 GHz masers (purple squares).
(A color version of this figure is available in the online journal.)

Since the 6.7 and 107 GHz transitions are both from the same family, a relationship between 6.7 GHz luminosity and the presence of a 107 GHz maser is perhaps not surprising; however, the degree of correlation between 6.7 and 107 GHz peak flux densities is lower than between 6.7 and 12.2 GHz. This figure also shows that the 37.7 GHz methanol masers are only present toward the most luminous 12.2 GHz methanol masers (those for which the 12.2 GHz peak luminosity is $\gtrsim$250 Jy kpc^2). The close relationship between the presence of a luminous 12.2 GHz maser and 37.7 GHz masers is likely due to the physical conditions required rather than some quirk

of the molecular quantum mechanics, as these two transitions are not in the same family, although both have their final state in the $K = -1$ tree of the E rotational species of methanol.

In general, we would expect the integrated luminosity of the maser emission to be a more reliable indicator of the physical conditions in a region as it depends on the conditions over a larger gas volume and will be less influenced by the stochastic nature of the maser process than is the case for a single spectral peak. We have undertaken the same analysis using the integrated 6.7 and 12.2 GHz maser luminosities and find that for the sources were data are available the same relationships are observed as seen in Figure 4. Unfortunately, integrated flux densities at 6.7 and 12.2 GHz are only available in the literature for approximately two-thirds of the 107 GHz methanol maser sample, whereas peak flux densities are available for all sources. For this reason we have chosen to show the peak luminosity relationship, rather than the equivalent plot for integrated luminosity.

We have looked at those 12.2 GHz methanol masers from the Breen et al. (2011a) sample for which the logarithm of their 6.7 GHz peak luminosity >2.9 and find that 90 of the 237 sources meet this criterion. Of these 45 have been searched for 107 GHz methanol masers by Caswell et al. (2000) or Val'tts et al. (1999), with maser emission detected toward 42% (we have counted those sources for which Caswell et al. (2000) suggested possible 107 GHz maser emission as masers for this purpose), and 107 GHz thermal emission detected toward a further 14%. Considering only the sources which also have the logarithm of their 12.2 GHz peak luminosity >2.4, there are 52 of 237 sources meeting these combined criteria. Of these only 15 have been searched for 37.7 GHz masers resulting in 8 detections (a detection rate of 53%). The class II methanol maser sources meeting the criteria outlined above which have not previously been searched for 107 and/or 37.7 GHz masers are clearly good targets for future searches in these transitions, as if similar detection rates are achieved it will result in a significant increase in the known number of sources for each of these transitions. We can use the information on the detection rates for the 107 and 37.7 GHz masers and the fraction of the total class II maser population that lie in the region of the 6.7–12.2 GHz peak luminosity plot favored by each of these transitions to estimate their lifetime by bootstrapping from the lifetime estimate of 6.7 GHz methanol masers of van der Walt (2005). Doing this we estimate the 107 GHz methanol maser phase lasts between 2 and 7 $\times$ 10^3 years and we infer a lifetime of 1–4 $\times$ 10^3 years for the 37.7 GHz transition. Working on the assumption that the interpretation of Breen et al. (2010), that the 6.7 and 12.2 GHz methanol maser luminosity increases as the sources evolve, is correct; the sources showing 107 GHz and in particular 37.7 GHz methanol masers are the most evolved sources traced by class II methanol masers and arise just prior to the switch off of class II methanol masers.

The results of Breen et al. (2010) suggest that the "turnoff" of class II methanol masers in star formation regions is a rapid one. The reason for this "turnoff" remains an open question. The modeling results of Cragg et al. (2005) suggest that the presence of the rare weak masers in more evolved sources is indicative of the physical conditions evolving toward those which favor a large number of methanol transitions. The sudden disappearance of the class II methanol masers, which reside very close to the protostar, suggests a catastrophic change in the environment of the masing gas. Possibilities include the conditions reaching a critical point where the methanol is rapidly depleted by gas-phase reactions, destruction of methanol by increased UV photon flux, or disruption of the velocity coherence in the masing gas by the passage of a shock front. Identifying these rare "post-peak-luminosity" class II methanol maser sources is likely to give us new insights into some of the critical factors governing the presence or otherwise of the masers. Figure 4 identifies one possible candidate for a post-peak-luminosity maser, in the form of the outlying 107 GHz methanol maser source G 192.600–0.048. This source is significantly less luminous at 12.2 GHz than the bulk of 107 GHz maser sources and also the least luminous at 6.7 GHz. Were it not that this source is relatively nearby (it is at a distance of 1.59 kpc, measured to an accuracy of better than 5% using parallax by Rygl et al. 2010), we would only be able to detect the 6.7 GHz methanol masers. Other candidates for post-peak-luminosity class II maser sources would be objects which have strong H II regions and low density (or high temperature), accompanied by a maser with a peak luminosity $\lesssim$1000 Jy pc^2.

5. CONCLUSIONS

We have undertaken a search for 37.7, 38.3, and 38.5 GHz class II methanol masers toward a large sample of 6.7 GHz methanol masers covering both the northern and southern hemispheres. This led to the detection of thirteen 37.7 GHz methanol masers, eight of which are new detections and the detection of three 38.3/38.5 GHz methanol masers, one of which is a new detection. We find that 37.7 GHz methanol masers are only detected toward the class II methanol maser sources which have the highest 6.7 and 12.2 GHz peak luminosities. In the developing maser-based evolutionary timeline, these sources are thought to signpost the latter stages of the class II methanol maser phase in star formation regions. We estimate that 37.7 GHz methanol masers have a lifetime of only a few thousand years and arise just prior to the changes which terminate methanol maser emission in the region, i.e., they are the horsemen of the apocalypse for the class II methanol maser phase.

S.P.E. thanks the Alexander-von-Humboldt-Stiftung for an Experienced Researcher Fellowship which has helped support this research. A.M.S. was partially supported by the Russian Foundation for Basic Research (grant nos. 10-02-00589, 11-02-01332, and 11-02-97124). We are grateful to L.E.B. Johansson and A.I. Vasyunin for help with the Onsala observations. The Mopra telescope is part of the Australia Telescope which is funded by the Commonwealth of Australia for operation as a National Facility managed by CSIRO. The OSO is the Swedish National Facility for Radio Astronomy and is operated by Chalmers University of Technology, Göteborg, Sweden, with nancial support from the Swedish Research Council and the Swedish Board for Technical Development. This research has made use of NASA's Astrophysics Data System Abstract Service.

REFERENCES

Batrla, W., Matthews, H. E., Menten, K. M., & Walmsley, C. M. 1987, Nature, 326, 49
Breen, S. L., Ellingsen, S. P., Caswell, J. L., et al. 2011a, ApJ, 733, 80
Breen, S. L., Ellingsen, S. P., Caswell, J. L., & Green, J. A. 2011b, MNRAS, submitted
Breen, S. L., Ellingsen, S. P., Caswell, J. L., & Lewis, B. J. 2010, MNRAS, 401, 221
Caswell, J. L. 1997, MNRAS, 289, 203

Caswell, J. L. 1998, MNRAS, 297, 215
Caswell, J. L. 2009, PASA, 26, 454
Caswell, J. L., Fuller, G. A., Green, J. A., et al. 2010, MNRAS, 404, 1029
Caswell, J. L., Fuller, G. A., Green, J. A., et al. 2011, MNRAS, 417, 1964
Caswell, J. L., Vaile, R. A., & Ellingsen, S. P. 1995a, PASA, 12, 37
Caswell, J. L., Vaile, R. A., Ellingsen, S. P., & Norris, R. P. 1995b, MNRAS, 274, 1126
Caswell, J. L., Vaile, R. A., Ellingsen, S. P., Whiteoak, J. B., & Norris, R. P. 1995c, MNRAS, 272, 96
Caswell, J. L., Yi, J., Booth, R. S., & Cragg, D. M. 2000, MNRAS, 313, 599
Cesaroni, R., & Walmsley, C. M. 1991, A&A, 241, 537
Cragg, D. M., Sobolev, A. M., Caswell, J. L., Ellingsen, S. P., & Godfrey, P. D. 2004, MNRAS, 351, 1327
Cragg, D. M., Sobolev, A. M., Ellingsen, S. P., et al. 2001, MNRAS, 323, 939
Cragg, D. M., Sobolev, A. M., & Godfrey, P. D. 2002, MNRAS, 331, 521
Cragg, D. M., Sobolev, A. M., & Godfrey, P. D. 2005, MNRAS, 360, 533
Ellingsen, S. P. 2006, ApJ, 368, 241
Ellingsen, S. P., Cragg, D. M., Lovell, J. E. J., et al. 2004, MNRAS, 354, 401
Ellingsen, S. P., Cragg, D. M., Minier, V., Muller, E., & Godfrey, P. D. 2003, MNRAS, 344, 73
Ellingsen, S. P., Norris, R. P., & McCulloch, P. M. 1996, MNRAS, 279, 101
Ellingsen, S. P., Voronkov, M. A., Cragg, D. M., et al. 2007, in IAU Symp. 242, Astrophysical Masers and their Environments, ed. J. M. Chapman & W. A. Baan (Cambridge: Cambridge Univ. Press), 213
Genzel, R., & Downes, D. 1977, A&AS, 30, 145
Green, J. A., Caswell, J. L., Fuller, G. A., et al. 2010, MNRAS, 409, 913
Green, J. A., & McClure-Griffiths, N. M. 2011, MNRAS, 417, 2500
Goedhart, S., Gaylard, M. J., & van der Walt, D. J. 2003, MNRAS, 339, 33
Goedhart, S., Minier, V., Gaylard, M. J., & van der Walt, D. J. 2005, MNRAS, 356, 839
Haschick, A. D., Baan, W. A., & Menten, K. M. 1989, ApJ, 346, 330
Koo, B., Williams, D. R. W., Heiles, C., & Backer, D. C. 1988, ApJ, 326, 931
Lo, K. Y., Burke, B. F., & Haskchick, A. D. 1975, ApJ, 220, 81
Malyshev, A. V., & Sobolev, A. M. 2003, Astron. Astrophys. Trans., 22, 1
Mehringer, D. M., Zhou, S., & Dickel, H. R. 1997, ApJ, 475, L57
Menten, K. M. 1991, ApJ, 380, L75
Minier, V., & Booth, R. S. 2002, A&A, 387, 179
Minier, V., Burton, M. G., Hill, T., et al. 2005, A&A, 429, 945
Minier, V., Ellingsen, S. P., Norris, R. P., & Booth, R. S. 2003, A&A, 403, 1095
Müller, H. S. P., Menten, K. M., & Mäder, H. 2004, A&A, 428, 1019
Pavlakis, K. G., & Kylafis, N. D. 1996a, ApJ, 467, 300
Pavlakis, K. G., & Kylafis, N. D. 1996b, ApJ, 467, 309
Reid, M. J., Menten, K. M., Zheng, X. W., et al. 2009, ApJ, 700, 137
Rygl, K. L. J., Brunthaler, A., Reid, M. J., et al. 2010, A&A, 511, 42
Slysh, V. I., Kalenskii, S. V., & Val'tts, I. E. 1995, ApJ, 442, 668
Sutton, E. C., Sobolev, A. M., Ellingsen, S. P., et al. 2001, ApJ, 554, 173
Szymczak, M., Hrynek, G., & Kus, A. J. 2000, A&AS, 143, 269
Urquhart, J. S., Hoare, M. G., Purcell, C. R., et al. 2010, PASA, 27, 321
Val'tts, I. E., Dzura, A. M., Kalenskii, S. V., et al. 1995, A&A, 294, 825
Val'tts, I. E., Ellingsen, S. P., Slysh, S. I., et al. 1999, MNRAS, 310, 1077
van der Walt, D. J. 2005, MNRAS, 360, 153
Vlemmings, W. H. T., Goedhart, S., & Gaylard, M. J. 2009, A&A, 500, 9
Voronkov, M. A., Brooks, K. J., Sobolev, A. M., et al. 2006, MNRAS, 373, 411
Walsh, A. J., Breen, S. L., Britton, T., et al. 2011, MNRAS, 416, 1764
Walsh, A. J., Macdonald, G. H., Alvey, N. D. S., Burton, M. G., & Lee, J.-K. 2003, A&A, 410, 597
Wang, Y., Beuther, H., Bik, A., et al. 2011, A&A, 527, 32
Wilson, T. L., Hüttemeister, S., Dahmen, G., & Henkel, C. 1993, A&A, 268, 249
Wilson, T. L., Walmsley, C. M., Menten, K. M., & Hermsen, W. 1985, A&A, 147, L19
Wilson, T. L., Walmsley, C. M., Snyder, L. E., & Jewell, P. R. 1984, A&A, 134, L7
Xu, L.-H., & Lovas, F. J. 1997, J. Phys. Chem. Ref. Data, 26, 17
Xu, Y., Li, J. J., Hachisuka, K., et al. 2008, A&A, 485, 729